

 <p><b>GKSS</b> FORSCHUNGSZENTRUM in der HELMHOLTZ-GEMEINSCHAFT</p>	<p><b>MERIS Lake Algorithm for BEAM</b></p>	<p>ATBD water Page 1 of 17 V 1.0, June 10, 2008</p>
---	---	---

## **Algorithm Theoretical Basis Document (ATBD)**

### **MERIS**

### **Lake Water Algorithm for BEAM**

Version 1.0, June 2008

Roland Doerffer & Helmut Schiller  
GKSS Forschungszentrum Geesthacht GmbH  
21502 Geesthacht

Development of MERIS lake water algorithms  
ESRIN Contract No. 20436/06/I-LG

	<b>MERIS Lake Algorithm for BEAM</b>	ATBD water Page 2 of 17 V 1.0, June 10, 2008
--	--	--

### Distribution

Name:

P. Regner (ESA / ESRIN)

S. Koponen

C. Brockmann

### Change Record

<u>Issue</u>	<u>Revision</u>	<u>Date</u>	<u>Description</u>
Draft 0.1	0	31.3.2007	Initial draft
V 1.0	0	10.9.2008	Final version

## *Table of Content*

<a href="#">Table of Content.....</a>	<a href="#">3</a>
<a href="#">Abstract.....</a>	<a href="#">4</a>
<a href="#">1Introduction.....</a>	<a href="#">4</a>
<a href="#">2Design of the Procedure.....</a>	<a href="#">5</a>
<a href="#">2.1Enhancement of the retrieval.....</a>	<a href="#">7</a>
<a href="#">2.2Special feature: cut off reflectance.....</a>	<a href="#">9</a>
<a href="#">3The bio-optical model.....</a>	<a href="#">9</a>
<a href="#">3.1Pure water.....</a>	<a href="#">10</a>
<a href="#">3.2Absorption by phytoplankton pigments.....</a>	<a href="#">10</a>
<a href="#">3.3Absorption by yellow substance.....</a>	<a href="#">10</a>
<a href="#">3.4Scattering and Absorption by total suspended matter in Finnish lakes.....</a>	<a href="#">10</a>
<a href="#">4Ranges.....</a>	<a href="#">11</a>
<a href="#">4.1Values and Ranges as defined in the simulation runs.....</a>	<a href="#">12</a>
<a href="#">4.2Environmental Conditions.....</a>	<a href="#">12</a>
<a href="#">4.3Calculation of the minimum irradiance attenuation coefficient <math>k_{min}</math> and the signal depth <math>z_{90}</math>.....</a>	<a href="#">13</a>
<a href="#">5Training of the NN.....</a>	<a href="#">13</a>
<a href="#">5.1Performance of the backward NN.....</a>	<a href="#">13</a>
<a href="#">6Bio-optical Model of Spanish Lakes used for the Eutrophic Lakes Processor.....</a>	<a href="#">14</a>
<a href="#">6.1Phytoplankton.....</a>	<a href="#">14</a>
<a href="#">6.2Total Suspended Matter TSM.....</a>	<a href="#">15</a>
<a href="#">6.3Yellow Substance.....</a>	<a href="#">15</a>
<a href="#">6.4Neural Network.....</a>	<a href="#">15</a>
<a href="#">6.5Performance of the backward NN.....</a>	<a href="#">16</a>
<a href="#">7References.....</a>	<a href="#">17</a>

## Abstract

The paper describes the lake water algorithms, which is a further development of the BEAM processor of the Medium Resolution Imaging Spectrometer (MERIS). The version described here is adapted to the bio-optical data, which were provided for the lakes in Finland and Spain. All bio-optical data were provided by the Finnish and Spanish partners of the project.

Input to the algorithms are the water leaving radiance reflectances of 8 MERIS bands. These data are the output of the atmospheric correction (s. atmospheric correction ATBD). The algorithms derive data of the inherent optical properties total scattering of particles (total suspended matter, tsm)  $b_{\text{tsm}}$ , the absorption coefficient of phytoplankton pigments  $a_{\text{pig}}$  and the absorption of dissolved organic matter  $a_{\text{gelb}}$  (gelbstoff), all at 443 nm (MERIS band 2). From these IOPs the concentrations of phytoplankton chlorophyll and of total suspended dry weight are determined. Furthermore, the attenuation coefficient for the downwelling irradiance,  $k$ , at the wavelength with maximum transparency is determined ( $k_{\text{min}}$ ) as well as the  $z_{90}$  signal depth, which indicates the water depth from which 90% of the reflected light comes from. The algorithm is based on a neural network (NN), which relates the bi-directional water leaving radiance reflectances with these concentration variables. The network is trained with simulated reflectances. The bio-optical model used for the simulations is based on a data set collected in different lakes in Finland and Spain.

Two NN's are trained with simulated reflectances:

1. *invNN* to emulate the inverse model  
(reflectances, geometry)  $\rightarrow$  concentrations, and
2. *forwNN* to emulate the forward model  
(concentrations, geometry)  $\rightarrow$  reflectances.

The *invNN* is used to obtain an estimate of the concentrations which is used as a first guess to start a minimization procedure, which uses the *forwNN* iteratively to minimize the difference between the calculated reflectances and the measured ones. The procedure is fast as it takes advantage of the Jacobian, which is a by-product of the NN calculation.

## 1 Introduction

Optical remote sensing of inland waters has become a task of increasing importance, since the availability of clean fresh water is one of the great environmental challenges. In particular natural lakes and artificial reservoirs have to be monitored on a regular basis to ensure the quality of the water. With its 300 m spatial resolution and 15 spectral bands the imaging spectrometer MERIS on ENVISAT can be used for monitoring of at least larger inland waters. However, the standard algorithms as used for open ocean or even coastal waters are not appropriate because different water constituents occur in particular different phytoplankton blooms with partly extreme high concentrations. Within this project two different algorithms have been developed to retrieve the concentrations from the water leaving radiance reflectances after atmospheric corrections. One for Boreal lakes, which are characterized by high concentrations of dissolved organic matter (humic acids) and another one for eutrophic lakes, which are often characterized by chlorophyll concentrations in the range of several hundred milligrams per cubic meter. Of particular importance is the detection

	<b>MERIS Lake Algorithm for BEAM</b>	ATBD water Page 5 of 17 V 1.0, June 10, 2008
---	--	--

and monitoring of cyanobacteria, because of their toxic character.

Both algorithms are based on neural network inverse modelling techniques. The training data sets are produced by radiative transfer simulations. The underlying bio-optical models are based on measurements in lakes of Finland for the Boreal Lake Processor (Kallio, Kari, 2008) and for the Eutrophic Lakes Processor on measurements in Spanish lakes and water reservoirs (Ruiz Verdú, Antonio, 2007, 2008).

## 2 Design of the Procedure

In the following we describe the procedure for the Boreal lakes processor, which are based on bio-optical data of Finland. Changes for the lakes of Spain (eutrophic lakes processor) are documented in chapter 6.

The NN transforms the directional water leaving radiance reflectances measured in eight spectral bands (outcome of the atmospheric correction procedure) and the three angles pixel by pixel with high efficiency into the three optical components, all at MERIS band 2, 443 nm:

- (1) absorption of phytoplankton pigments,  $a_{\text{pig}}$ ,
- (2) the scattering of all particles (total suspended matter, tsm)  $b_{\text{tsm}}$ ,
- (3) the absorption of dissolved organic material  $a_{\text{gelb}}$ , which is defined as the absorption of all matter, which passes a filter with a pore size of 0.2  $\mu\text{m}$ .

The chlorophyll concentration is then determined from its relationship between absorption  $a_{\text{pig}}$  and concentration, and the dry weight of the total suspended matter from its relationship between  $b_{\text{tsm}}$ .

The directional water leaving radiance reflectance  $RLW(\theta_v, \phi_v)$  associated with the water leaving radiance  $L_w(\theta, \phi)$  and the downwelling irradiance above the sea surface  $E_d$  is defined to be:

$$RLW(\theta_v, \phi_v) = L_w(\theta_v, \phi_v) / E_d(\theta_s)$$

where  $\theta_v$  and  $\phi_v$  are the zenith and azimuth observation angles respectively.  $E_d$  depends on the solar zenith angle,  $\theta_s$ , for the pixel under examination. For convenience we will denote the wavelength dependency in the following chapters only where necessary.

Since simultaneous measurements of concentrations and water leaving radiance reflectance spectra are rare and, thus, do not cover the data space with sufficient density, the construction of the NN is based on a large table (> 80 000 entries) of simulated data generated by our forward model, which is a special version of the HYDROLIGHT radiative transfer code (Mobley 1994), plus the bio-optical model relating scattering and absorption coefficients to concentrations.

This bio-optical model is based on a data set of measurements of inherent optical properties and describes the variability of the three major components of lake waters, i.e. scattering by all particles and the absorption after bleaching, absorption by phytoplankton pigments and absorption by humic organic matter (*gelbstoff*).

For given concentrations / IOPs of water constituents the forward model calculates the

angular distribution of water leaving radiance in 12 MERIS bands. These angular distributions are sampled in the appropriate angle ranges to derive the entries of the training / test tables for building the NN: three IOPs, three angles and 8 (out of 12) water leaving radiance reflectances. For the simulation the concentrations of the 3 water constituents are randomly sampled from a logarithmic distribution in order to disentangle small concentration differences in regions of small concentrations. In order to get roughly constant relative concentration errors the logarithm of the concentrations was also used as NN output.

To avoid extrapolation from the training set the NN has to learn the variability of the inherent optical properties (IOP) of the water constituents as well as the errors in reflectances caused by the instrument and the atmospheric correction. Thus, the natural variability of the IOPs was built into the forward model by sampling the parameters describing the spectral dependence of the IOPs from their measured distributions (s. details in bio-optical model chapter).

Two NN's are trained (Schiller, 2000) with this table: (1) *invNN* to emulate the inverse model  $\mathbf{c} = F_g^{-1}(\mathbf{r})$  from reflectances  $\mathbf{r}$  and geometry information  $\mathcal{G}$ , and (2) *forwNN* to emulate the forward model  $\mathbf{r} = F_g(\mathbf{c})$  deriving reflectances  $\mathbf{r}$  from concentrations  $\mathbf{c}$  and geometry information  $\mathcal{G}$ .

In the MERIS ground segment (Schiller and Doerffer, 1999, Doerffer & Schiller, 2007) the two NN's are combined to give a new NN (s. Fig. 1), which first uses the *invNN* part to obtain an estimate of the concentrations  $\mathbf{c}$ . These together with the geometry information  $\mathcal{G}$  are fed into the *forwNN*. If not only the measurement of the reflectances but also the model is perfect the identity  $\mathbf{r} = F_g(F_g^{-1}(\mathbf{r}))$  should hold. Therefore the reflectances  $\mathbf{r}'$  returned by the *forwNN* are compared with the measured ones. Large deviations signal a violation of the necessary condition for a successful inversion; corresponding pixels are then flagged (Doerffer and Schiller, 2000)).

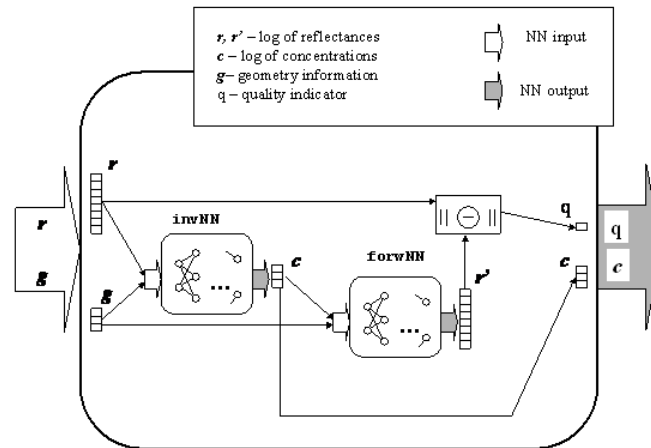


Fig. 1: A combination of NN's is used in the MERIS ground segment for the retrieval of water

A combination of NN's is used in the MERIS ground segment for the retrieval of water constituent concentrations  $\mathbf{c}$  from remotely sensed reflectances  $\mathbf{r}$  and geometry information  $\mathbf{g}$ . The  $\mathbf{c}$  obtained from the *invNN* emulating the inverse model is used together with the geometry information  $\mathbf{g}$  as input to the *forwNN* which calculates the corresponding reflectances  $\mathbf{r}'$  which are compared with the measured ones to give a quality measure  $q$  of the retrieval.

## 2.1 Enhancement of the retrieval

The advanced algorithm (Schiller and Doerffer, 2005) is depicted in fig. 2. Now after the comparison of the reflectances  $\mathbf{r}'$  returned by the *forwNN* with the measured ones, optimization steps are inserted. The aim is to improve the agreement of  $\mathbf{c}$  with  $\mathbf{r}$  by iteratively adjusting the estimate of  $\mathbf{c}$ .

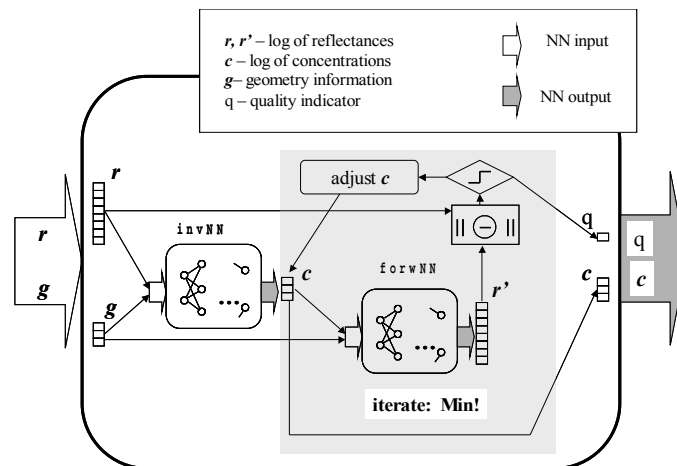


Fig. 2: In the enhanced algorithm the optimization loop replaces the simple quality check.

We apply the Levenberg-Marquardt minimization algorithm which reads for our problem like follows:

The error sum to be minimized is  $(\mathbf{r}' - \mathbf{r})^2 / 2$ . We have an estimation of  $\mathbf{c}$ . Application of the NN not only allows to get  $\mathbf{r}' = \text{forwNN}(\mathbf{c})$  but also to calculate the Jacobi matrix  $\mathbf{Z}_{ni} = \frac{\partial r'_n}{\partial c_i}$ .

The new estimate is  $\mathbf{c}_{new} = \mathbf{c}_{old} - (\mathbf{Z}^T \mathbf{Z} + \lambda \mathbf{I})^{-1} \mathbf{Z}^T (\mathbf{r}'(\mathbf{c}_{old}) - \mathbf{r})$ . If the resulting error is less than the old one the new estimate is accepted and the next iteration step is done with  $\lambda \leftarrow \lambda / 20$ . Otherwise the trial is repeated with  $\lambda \leftarrow \lambda \times 20$ . (At the very beginning  $\lambda = 0.01$ ). We stop the optimization loop after at most 10 iterations or if the relative error change is less than 3% or if all parameters change  $< 0.005$ .

In summary the algorithm development consists of the following steps:

- Set up of a bio-optical model based on measurements of IOPs and concentrations including the natural variability of IOPs
- Definition of the range of concentrations and further boundary conditions (s. bio-optical model)
- Estimation of expected errors of RLW's based on instrumental errors and uncertainties of atmospheric correction
- Simulation of RLW spectra
- Training of the NN's
- Test of the NN's
- Use of the NN's within the processor
- Validation of the algorithm and the products

	<b>MERIS Lake Algorithm for BEAM</b>	ATBD water Page 9 of 17 V 1.0, June 10, 2008
--	--	--

## 2.2 Special feature: cut off reflectance

A special feature is the cut-off reflectance. The  $RL_w$ , which are retrieved from the top of atmosphere radiances by the atmospheric correction procedure can be significantly inaccurate or even negative at low reflectances, e.g. in the red part of the spectrum in case 1 waters due to the high absorption of pure water or in the blue part in case of high concentrations of yellow substances. Since we use the logarithm of the reflectances even small absolute errors of these bands can degrade the performance of the NN significantly. In order to cope with such faulty input the NN was trained in such a way that the reflectance was set to  $\log(RL_w)$  of  $-6.9 \text{ sr}^{-1}$  whenever the reflectance is below this minimum. Accordingly the measured reflectances after atmospheric correction were treated in the same way. However a minimum of 3 bands with reflectances above this threshold is required to run the NN algorithm. This cut off feature improved the results significantly, because low reflectances data with a relative high noise or negative reflectances are excluded.

In a new version of the atmospheric correction procedure (s. corresponding ATBD) negative reflectances cannot longer occur. In this case it is not necessary to determine the cut off reflectance. Only the limits of the NN are tested, i.e. if  $RL_w < \text{NN input minimum}$  or  $> \text{NN input maximum}$ , the minimum or maximum is used and an “out of range flag” is raised.

## 3 The bio-optical model

Lake water constituents comprise a large number of different substances, which include mineralic dissolved and particulate compounds, a large variety of organic macromolecules, living organisms such as phytoplankton, zooplankton, bacteria etc., and their debris and excrements. All of these water constituents have different optical properties concerning scattering and absorption and partly fluorescence.

For the purpose of optical remote sensing this diversity of substances has to be grouped into a small number of classes each of which includes constituents with similar optical properties and / or correlated concentrations. For the majority of the world ocean areas it is sufficient to comprise all substances into one group using phytoplankton chlorophyll *a* as a proxy for its concentration. This type of water is called case I water. The concentration of this class of substances - in terms of chlorophyll *a* - can be derived from the blue to green shift of the water colour. In many coastal waters as well as in lake and river waters one needs more than one class of substances to describe the variability of water colour. By tradition and experience three classes are defined: (1) phytoplankton pigment with chlorophyll *a* as a proxy, (2) the dry weight of all particles (total suspended matter, TSM) and (3) the absorption caused by the "dissolved" fraction of all water constituents (*gelbstoff*).

However, each of the three groups of substances is variable with respect to their composition and thus their chemical, physical and in particular optical properties. Any remote sensing system and retrieval algorithm has to take this variability into account.

An overview of all components as defined for the Finnish lakes with their properties is given in table 1.

The components are defined according to the separation and measurement procedures. One critical issue is the separation of the absorption of phytoplankton pigments and the absorption of other substances, which are part of suspended matter. This separation is performed by bleaching of the TSM using NaHCl. The difference in the absorption spectrum before and

after this bleaching treatment is assumed to be the absorption of all phytoplankton pigments. Another issue is the separation between dissolved yellow substance and the absorption of TSM, which is determined by the type and pore size of the filter used for separation, which traditionally was 0.45  $\mu\text{m}$  and nowadays is 0.2  $\mu\text{m}$ .

### 3.1 Pure water

The absorption of pure water is based on the measurements of Pope and Fry (1997), the scattering of pure water on the formulation of Morel (1974).

### 3.2 Absorption by phytoplankton pigments

The absorption spectrum of phytoplankton pigments was determined as a function of the concentration for each wavelength, i.e. the relationship between chlorophyll concentration and absorption is described by an exponential function of the type:

$$a_{Ph}^*(\lambda) = A(\lambda) C_{Chl}^{-B(\lambda)}$$

A and B are coefficients which were provided as a table for the wavelength range 400-750 nm with 2 nm resolution. Absorption spectra for the MERIS bands for different concentrations are plotted in Fig. 3.

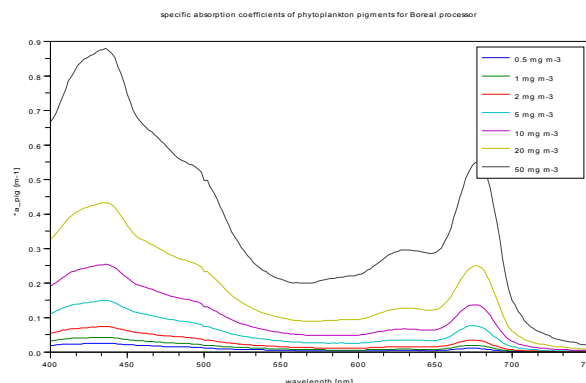


Fig. 3: Absorption spectra of phytoplankton of Finnish lakes

### 3.3 Absorption by yellow substance

Yellow substance  $a_{\text{gelb}}$  is defined here as the absorption at 443 nm of all water constituents which pass a Millipore filter with a pore size of 0.2  $\mu\text{m}$ . The wavelength exponent of the quasi exponential decrease of absorption with increasing wavelength was determined as

$$S_{\text{CDOM}} = 0.016 \pm 0.0015 \text{ nm}^{-1}$$

### 3.4 Scattering and Absorption by total suspended matter in Finnish lakes

Particles are defined as all substances, which remain on a filter with a pore size of 0.45  $\mu\text{m}$ .

The absorption properties are determined after deterioration of the phytoplankton pigments using NaHCl. These absorption spectra look very similar to those of yellow substance but

	<b>MERIS Lake Algorithm for BEAM</b>	ATBD water Page 11 of 17 V 1.0, June 10, 2008
--	--	---

with a lower wavelength exponent. This exponent was determined in the same way as that of yellow substance. For Finnish lakes it is

$$S_{bTSM} = 0.010 \pm 0.001 \text{ nm}^{-1}.$$

The spectral dependence of for total suspended matter scattering was determined as:

$$b_{TSM}^*(\lambda) = b_{TSM}^*(443) \left( \frac{443}{\lambda} \right)^{n_b}$$

with an exponent  $n_b = 0.705$

The relationship between dry weight concentration and absorption and scattering was determined as:

$$a_{bTSM}^*(443) = 0.089 \text{ m}^2 \text{ g}^{-1} \pm 0.047 \text{ m}^2 \text{ g}^{-1}$$

$$b_{TSM}^*(443) = 0.96 \text{ m}^2 \text{ g}^{-1} \pm 0.28 \text{ m}^2 \text{ g}^{-1}$$

## 4 Ranges

The range of concentrations and / or optical properties was set according to the measurements in Finnish lakes.

Concentration range of Chl-a + Phae-a is 0.5 – 50 ug l<sup>-1</sup>, occasionally up to 90 ug l<sup>-1</sup> (in 4% of the measured cases concentration was between 41 and 90 ug l<sup>-1</sup>).

$a_{CDOM}(440)$  range is 0.25 – 10 m<sup>-1</sup>, occasionally up to 17 m<sup>-1</sup> (in 4% of the measured cases  $a_{CDOM}(440)$  was between 12 and 17 m<sup>-1</sup>).

Concentration range of TSM is 0.1 – 20 mg l<sup>-1</sup>, occasionally up to 40 mg l<sup>-1</sup> (in 4% of the measured cases concentration was between 15 and 40 mg l<sup>-1</sup>).

#### 4.1 Values and Ranges as defined in the simulation runs

<i>Component / property</i>	<i>value range</i>
Gelbstoff absorption wavelength exponent	0.016
Bleached particle absorption wavelength exponent	0.010
Particle scattering wavelength exponent	0.705
White particle scattering wavelength exponent	0.0
Phytoplankton pigment absorption	According to the table which relates absorption to chlorophyll concentration for each wavelength separately
Gelbstoff absorption $a_{\text{gelb}}$ at 442 nm	0.25 - 10.0 m <sup>-1</sup>
TSM concentration	0.1 - 20.0 mg l <sup>-1</sup>
White particle scattering $bpw$ at 442 nm	0.001 - 0.01 m <sup>-1</sup>
Phytoplankton chlorophyll concentration	0.5 - 50.0 $\mu\text{g l}^{-1}$
Sun zenith angle	0 - 80 degree
Viewing zenith angle	0 - 50 degree
Difference between sun and viewing azimuth angle	0 - 180 degree

Table 1: Optical properties and range used for the simulation of water leaving radiance reflectance spectra of Finnish lakes

#### 4.2 Environmental Conditions

The environment as well as further optical properties were defined in the following way: infinite deep water (no bottom effect), vertical homogeneous distribution of all water constituents, rough water surface according to a wind speed of 3 ms<sup>-1</sup>.

The downwelling radiance distribution above water has been simulated with Hydrolight, which was adapted for this purpose to simulate an atmosphere with 50 layers for 17 solar zenith angles ranging from 0 to 80 degree.

Furthermore no inelastic scattering (fluorescence or Raman scattering) as well as no polarisation effects have been considered in the simulation for the water retrieval algorithm (but see atmospheric correction ATBD).

### **4.3 Calculation of the minimum irradiance attenuation coefficient $k_{min}$ and the signal depth $z_{90}$**

The downwelling irradiance attenuation coefficient  $k$  is computed for each MERIS band using the two-flow approximation  $k = \sqrt{a_{tot}(a_{tot} + 2 * bb_{tot})}$ , with  $a_{tot}$  the total absorption coefficient, i.e. of water, pigments and yellow substance including bleached particles, and  $bb_{tot}$  is the backscattering coefficient of pure water and all particles in water. The backscattering coefficient is computed from the scattering coefficients. For water 0.5 of the scattering coefficient according to the Rayleigh phase function is used. For the particles we use a backscattering factor of 0.05, which is larger than the backscattering factor of 0.015 as determined from the phase function used in the model. Reason is that one has to take the shape factor into account, which we assume in the order of  $\pi$ .

The concentrations of total suspended matter dry weight (tsm) and of phytoplankton chlorophyll is determined from the IOPs as output of the neural network and the conversion relationships as provided by Kallio (2008):

$$\text{Chl} = 62.6 * a_{pig}(443)^{1.29} [\text{mg m}^{-3}]$$

$$\text{TSM} = 1.042 * b_{TSM}(443)$$

The minimum attenuation coefficient  $k_{min}$  is computed as the mean of the  $k$  values of those three bands with the smallest  $k$  values.

The signal depth  $z_{90}$  is estimated simply as  $1/k_{min}$ . It is given in negative numbers to produce a low (dark) grey level in images for water with a large signal depth and a bright grey level for waters with a small signal depth.

## **5 Training of the NN**

Using the bio-optical model as described above 8700 cases with different sun elevation, TSM and chlorophyll concentration and yellow substance absorption have been computed using Hydrolight. For each of these cases 7 viewing directions were randomly chosen so that all together > 60 000 spectra were used for training and testing.

### **5.1 Performance of the backward NN**

The performance of the NN are tested by using the simulated Rlw of the test data set as input to the NN. The following scatter plots show the results of the output of the NN compared to the expected values as used in the radiative transfer model to simulate the Rlw.

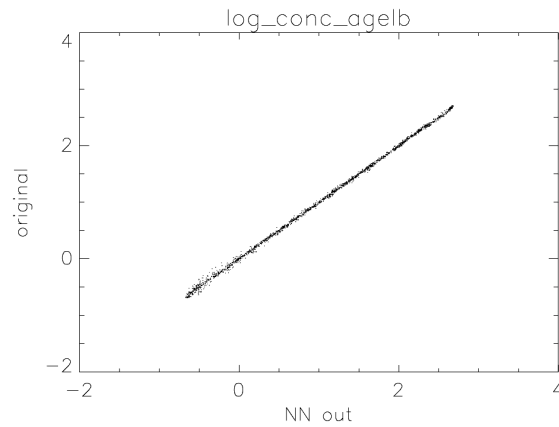


*Fig. 4: Test of the NN for absorption of yellow substances*

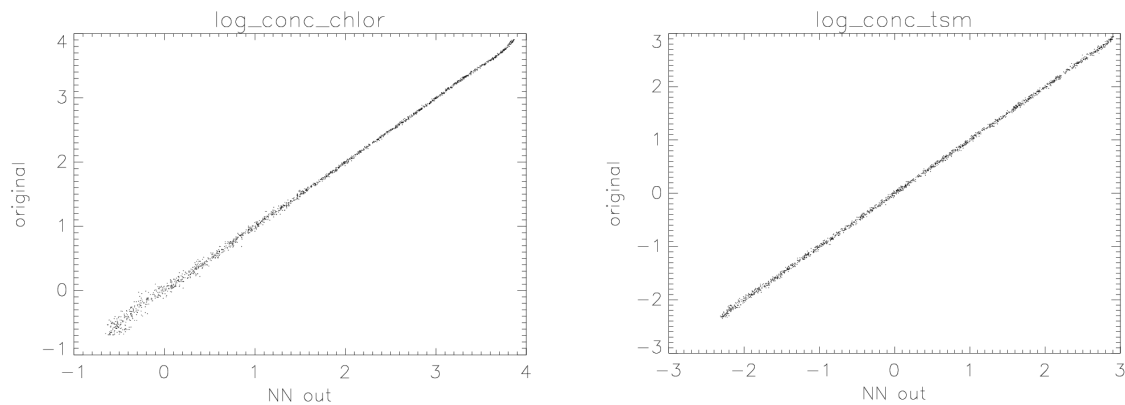


*Fig. 5: Test of the NN for absorption of chlorophyll (left) and TSM (right)*

## 6 Bio-optical Model of Spanish Lakes used for the Eutrophic Lakes Processor

### 6.1 Phytoplankton

The water processor for the Spanish lakes (Eutrophic Lakes Processor) is similar to the one for the Boreal Processor. However, one problem is the high amount of phycocyanin for lakes with high concentrations of cyanobacteria. With the presently available data it was not possible to split the pigment fraction into 2 components, as required to determine phycocyanin independently from chlorophyll. Thus one mean spectrum of the specific absorption was used with following values per mg chlorophyll  $\text{m}^{-3}$  of water:

MERIS band (nm): 412.0, 442.0, 490.0, 510.0, 555.0, 560.0, 620.0, 664.0, 670.0, 708.0, 753.0, 778.0, 865.0

absorption  $\text{a m}^{-1}$  : 0.0255, 0.0318, 0.0241, 0.0174, 0.00914, 0.00914, 0.0150, 0.0233, 0.0233, 0.00300, 0.000024, 0.00001, 0.000001

The range was set to: 1 – 120  $\text{mg m}^{-3}$

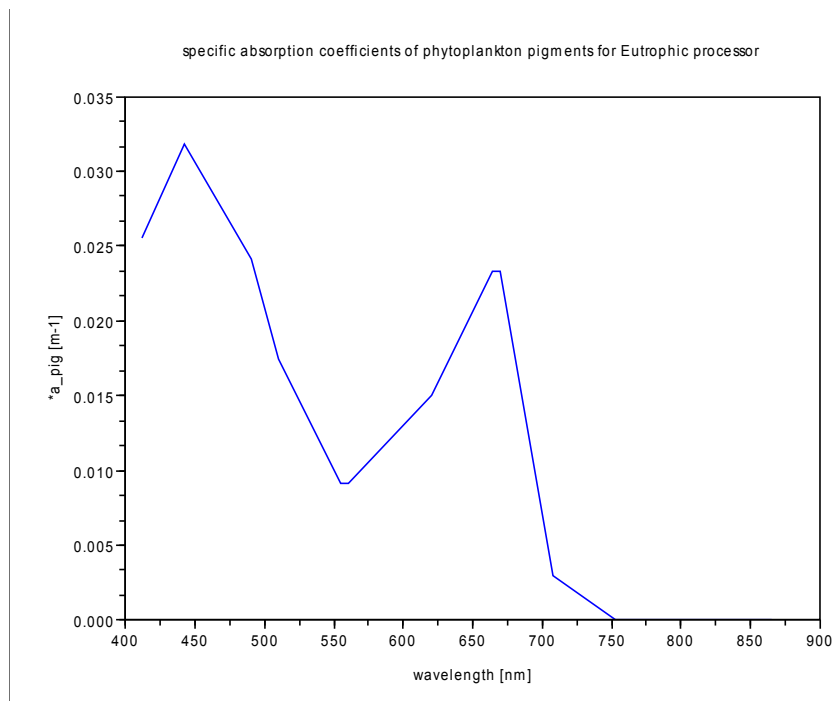


Fig. 6: Specific absorption coefficients used for Eutrophic Lake Processor

## 6.2 Total Suspended Matter TSM

TSM is characterized by scattering. For the scattering wavelength exponent the same values as for the Boreal lakes of 0.705 was taken.

For the range values between  $b = 0.25 \text{ m}^{-1}$  and  $30.0 \text{ m}^{-1}$  were taken.

As conversion factor the value from the coastal water processor was taken

$$\text{TSM} [\text{g m}^{-3}] = 1.7 b_{\text{tsm}443}$$

## 6.3 Yellow Substance

The yellow substance was split into two independent components:

- fulvic acids with a wavelength exponent of 0.022
- humic acids with a wavelength exponent of 0.008

The range was set for both components to  $a_{443} : 0.1 - 3.0 \text{ m}^{-1}$

## 6.4 Neural Network

Two NNs have been trained. The forward NN is 30x15\_88.8forw.net, and the backward 60x20\_586.8inv.net.

Input to the NN are the MERIS bands 2-7, 9 and the three angles (sun and viewing zenith and azimuth difference). Band 1 (412 nm) was omitted due to the uncertainties in calibration. Later tests have shown that for the new atmospheric correction procedure the band could return, as done for the Boreal Lake processor.

Output of the NN are:

- chlorophyll concentration in the range 1-120 mg m<sup>-3</sup>
- total suspended matter dry weight in the range 0.42 – 50.9 g m<sup>-3</sup>
- absorption coefficient of the fulvic acid component with a wavelength exponent of 0.22 in the range  $a_{442}$  0.1 – 3.0
- absorption coefficient of the humic acid component with a wavelength exponent of 0.008 in the range  $a_{442}$  0.1 – 3.0

Furthermore the following related variables are computed:

- $a_{pig}$ , which is the chlorophyll concentration \* 0.0318
- $b_{tsm}$ , which is the TSM concentration divided by 1.7
- $a_{tot}$
- $z_{90\_max}$  in meter
- $k_{max}$  in 1/meter

## 6.5 Performance of the backward NN

The performance of the NN are tested by using the simulated RIw of the test data set as input to the NN. The following scatter plots show the results of the output of the NN compared to the expected values as used in the radiative transfer model to simulate the RIw.

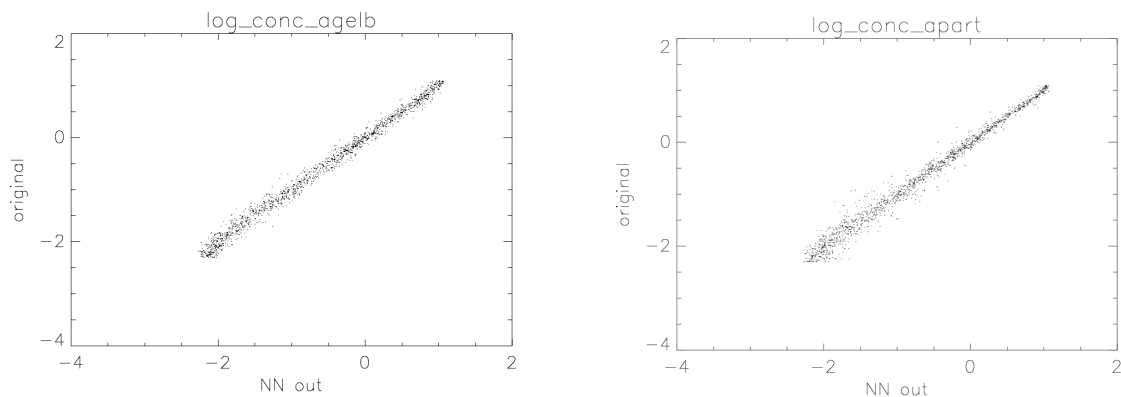


*Fig. 7: Test of the NN for absorption of fulvic acids (left) and humic acids (right)*

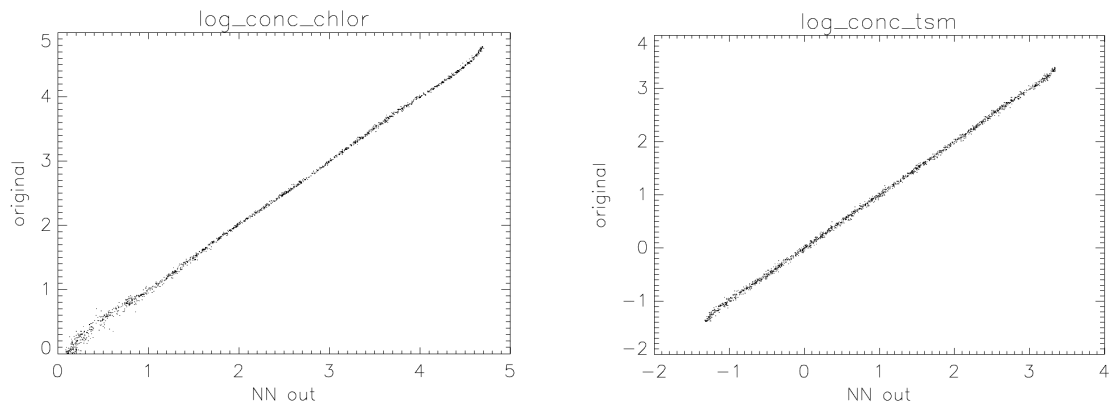


*Fig. 8: Test of the NN for absorption of chlorophyll (left) and TSM (right)*

## 7 References

- R. Doerffer and H. Schiller, 2000, Neural Network for Retrieval of Concentrations of Water Constituents with the Possibility of Detecting Exceptional out of Scope Spectra. Proc. IGARSS 2000, pp. 714-717.
- Mobley, C. D. 1994, Light and Water Radiative Transfer in Natural Waters. Academic Press, Inc.
- Kallio, Kari (2008): New SIOPs for Finnish lakes (2008), Technical Note, March 26, 2008, Syke, kari.y.kallio@ymparisto.fi
- Morel, A., 1974, Optical Properties of pure water and sea water. In Optical aspects of oceanography, ed. By N. G. Jerlov and Nielsen, E. S., pp 1-24, Academic New York.
- Morel, A. and D. Antoine, 2000, ATBD 2.9: Pigment Index Retrieval in Case 1 Waters. ESA Doc. No. PO-TN-MEL-GS-0005, pp. 9-1 - 9-26; it can be downloaded from [http://isat.esa.int/instruments/meris/pdf/atbd\\_2\\_09.pdf](http://isat.esa.int/instruments/meris/pdf/atbd_2_09.pdf).
- Petzold, T. L., 1972, Volume scattering functions for selected ocean waters. San Diego: Scripps Inst. Oceanogr., Ref 72-78, 79pp.
- Pope, R. and E. Fry, 1997, Absorption spectrum (380-700nm) of pure waters: II. Integrating cavity measurements, Applied Optics, pp 8710-8723.
- Ruiz Verdú, Antonio (2007, 2008) Bio-optical data of Spanish Lakes, provided to the Lake Project
- Schiller, H. and R. Doerffer, 1999, Neural Network for Emulation of an Inverse Model - Operational Derivation of Case II Water Properties from MERIS data. Int. J. Remote Sensing, vol. 20, pp. 1735-1746.
- Schiller, H., 2000, Feedforward-Backpropagation Neural Net Program ffbp1.0. Report GKSS 2000/37, ISSN 0344-9626.
- Schiller, H. and R. Doerffer, 2005, Improved Determination of Coastal Water Constituent Concentrations from MERIS Data, IEEE transactions on geoscience and remote sensing, vol 43, pp. 1585-1591, 2005.